



**Manuscript version: Author's Accepted Manuscript**

The version presented in WRAP is the author's accepted manuscript and may differ from the published version or Version of Record.

**Persistent WRAP URL:**

<http://wrap.warwick.ac.uk/104471>

**How to cite:**

Please refer to published version for the most recent bibliographic citation information. If a published version is known of, the repository item page linked to above, will contain details on accessing it.

**Copyright and reuse:**

The Warwick Research Archive Portal (WRAP) makes this work by researchers of the University of Warwick available open access under the following conditions.

Copyright © and all moral rights to the version of the paper presented here belong to the individual author(s) and/or other copyright owners. To the extent reasonable and practicable the material made available in WRAP has been checked for eligibility before being made available.

Copies of full items can be used for personal research or study, educational, or not-for-profit purposes without prior permission or charge. Provided that the authors, title and full bibliographic details are credited, a hyperlink and/or URL is given for the original metadata page and the content is not changed in any way.

**Publisher's statement:**

Please refer to the repository item page, publisher's statement section, for further information.

For more information, please contact the WRAP Team at: [wrap@warwick.ac.uk](mailto:wrap@warwick.ac.uk).

# Enhanced differentiation potential of primary human endometrial cells cultured on 3D scaffolds

*Ahmed M. Eissa, <sup>\*,†,‡,§,||</sup> Flavio S. V. Barros,<sup>⊥</sup> Pavle Vrljicak,<sup>⊥</sup> Jan J. Brosens<sup>\*,⊥</sup> and Neil R. Cameron<sup>\*,†,§</sup>*

<sup>†</sup> School of Engineering, University of Warwick, Coventry, CV4 7AL, U.K.

<sup>‡</sup> Department of Chemistry, University of Warwick, Coventry, CV4 7AL, U.K.

<sup>§</sup> Department of Materials Science and Engineering, Monash University, Clayton, 3800, Victoria, Australia.

<sup>||</sup> Department of Polymers, Chemical Industries Research Division, National Research Centre (NRC), El Bohouth St. 33, Dokki, Giza, 12622, Cairo, Egypt.

<sup>⊥</sup> Division of Biomedical Sciences, Reproductive Health Unit, Clinical Science Research Laboratories, Warwick Medical School, University of Warwick and Tommy's National Centre for Miscarriage Research, University Hospitals Coventry and Warwickshire NHS Trust, Coventry, CV2 2DX, U.K.

ABSTRACT

Novel approaches for culturing primary human cells *in vitro* are increasingly needed to study cell and tissue physiology and to grow replacement tissue for regenerative medicine. Conventional 2D monolayer cultures of endometrial epithelial and stromal cells fail to replicate the complex 3D architecture of tissue. A fully synthetic scaffold that mimics the microenvironment of the human endometrium can ultimately provide a robust platform for investigating tissue physiology and, hence, take significant steps towards tackling female infertility and IVF failure. In this work, emulsion-templated porous polymers (known as polyHIPEs) were investigated as scaffolds for the culture of primary human endometrial epithelial and stromal cells (HEECs and HESCs). Infiltration of HEECs and HESCs into cell-seeded polyHIPE scaffolds was assessed by histological studies, and phenotype was confirmed by immunostaining. Confocal microscopy revealed that the morphology of HEECs and HESCs is representative of that found *in vivo*. RNA sequencing was used to investigate transcriptome differences between cells grown on polyHIPE scaffolds and in monolayer cultures. The differentiation status of HEECs and HESCs grown in polyHIPE scaffolds and in monolayer cultures was further evaluated by monitoring the expression of endometrial marker genes. Our observations suggest that a 3D cell culture model that could approximate native human endometrial architecture and function can be developed using tailored polyHIPE scaffolds.

## INTRODUCTION

Impaired interaction between the endometrium and embryo leads to implantation failure, infertility, miscarriage, fetal growth restriction and preterm birth. These disorders are the leading cause of fetal loss and neonatal morbidity and mortality. Early embryo implantation events are

highly species-specific.<sup>1</sup> Studies in murine models have revealed that implantation is a step-wise process involving apposition of the embryo to the luminal endometrial epithelium, followed by adhesion and then invasion into the underlying stroma. Human embryo implantation is a complex process comprising a highly co-ordinated crosstalk between the embryo and the uterus, as well as communication amongst the different cellular constituents of the endometrium, including local immune cell populations. Due to ethical restrictions, implantation events cannot be studied directly in humans. *In vitro* culture of human endometrial cells would allow the study of endometrial function. Typically, endometrial stromal and epithelial cell functions are studied *in vitro* using standard two dimensional (2D) monolayer cultures, which fail to recapitulate the complex 3D architecture of the endometrium *in vivo*. For instance, it has been a challenge to maintain long-term functional human endometrial epithelial cells (HEECs) that mimic the *in vivo* responses to differentiation and proliferation signals.<sup>2</sup> Once in monolayer culture, HEECs rapidly undergo proliferation arrest and become senescent.<sup>3</sup> Furthermore, they lose their specialised properties, a process known as dedifferentiation, and become unresponsive to ovarian steroid hormones.<sup>4</sup> Therefore, there is an unmet need in reproductive medicine for technologies that support 3D endometrial cell growth *in vitro* and hence allow development of fully functional 3D endometrial construct that is more representative of *in vivo* human tissue.

Due to their high porosity, high permeability and tuneable mechanical properties, emulsion-templated porous polymer scaffolds are attractive materials for 3D cell culture and tissue engineering. The droplets of a polymerizable high internal phase emulsion (HIPE) become interconnected upon curing, producing a fully interconnected porous polymer known as a polyHIPE. The pore diameter and properties of these materials can be tailored to a high extent, making them suitable for 3D cell culture, tissue engineering and regenerative medicine.<sup>5, 6</sup> An

interesting approach has been reported recently that involves combining hard sphere and high internal phase emulsion templating to produce multi-level hierarchically porous materials with an interconnected porous topology. The suitability of this material to support the growth and proliferation of human osteoblast cells has been also shown.<sup>7</sup>

Recently, degradable polyHIPE materials have been prepared by photochemical thiol-ene polymerisation employing commercially available monomers.<sup>8</sup> The resulting scaffolds are chemically similar to common biomaterials, such as polylactide and polycaprolactone, and degrade by similar mechanisms (ester hydrolysis).<sup>9, 10</sup> Importantly, the degradation products are non-toxic (L929 fibroblast cell culture assay), easily excreted small molecules.<sup>10</sup> The compression Young's modulus of these polyHIPE materials ranges from highly elastic (0.2 kPa) to highly rigid (84.3 kPa).<sup>11</sup> The scaffolds have been shown to support 3D growth of a wide range of cell types.<sup>9, 12, 13</sup>

Establishment of a 3D model of human endometrium to study normal and pathological embryo-maternal interactions has the potential to accelerate the development of novel treatment strategies for female infertility and miscarriage prevention. Our work therefore aims to establish 3D endometrial cell growth in polyHIPE scaffolds. We show that these scaffolds support the growth of primary human stromal and epithelial endometrial cells, HESCs and HEECs, respectively. Cell infiltration was investigated by Hematoxylin and Eosin (H&E) staining and phenotype confirmed by immunostaining. Cell morphology was studied by confocal microscopy and impact on cell function was assessed by expression of marker genes and genome-wide expression profiling using RNA-sequencing. All experiments were carried out in comparison to conventional 2D monolayer cultures.

## EXPERIMENTAL SECTION

### Materials

All reagents and solvents used in polyHIPE synthesis were obtained at the highest purity available from Sigma-Aldrich and used without further purification, apart from the surfactant Hypermer B246 (a block copolymer of polyhydroxystearic acid and polyethylene glycol), which was obtained from Croda International.

### PolyHIPE Preparation and Characterisation

The preparation of polyHIPE materials by emulsion templating and photopolymerisation has already been reported.<sup>11</sup> Briefly, in a 250 mL two-necked round-bottomed flask, an oil phase consisting of the monomers trimethylolpropane tris(3-mercaptopropionate) (TMPTMP) (4.84 g) and dipentaerythritol penta-/hexa-acrylate (DPEHA) (3.47 g) plus 1,2-dichloroethane (DCE) (7 mL), surfactant Hypermer B246 (0.47 g) and a photoinitiator (a blend of diphenyl(2,4,6-trimethylbenzoyl)phosphine oxide and 2-hydroxy-2-methylpropiophenone) (0.7 mL) was stirred continuously at ambient temperature using a D-shaped polytetrafluoroethylene (PTFE) paddle attached to an overhead stirrer at 350 rpm. An aqueous phase of deionised water (70 mL) was added dropwise to the oil phase, with stirring, to form a HIPE with an internal (aqueous) phase volume fraction of 80%. Once all the aqueous phase was added, the HIPE was transferred immediately into a cylindrical PTFE mould (diameter 15 mm, depth 30 mm). The mould was secured between two glass plates and passed under a UV irradiator (Fusion UV Systems Inc. Light Hammer® 6 variable power UV curing system with LC6E benchtop conveyor) ten to fifteen times

on each side, at a belt speed of 5.0 m/min., to ensure complete curing. The cured polyHIPE material was washed by immersion in acetone and then soxhlet extraction with dichloromethane for 24 h to ensure complete removal of any residual thiol or acrylate monomers. The polyHIPE was then dried under reduced pressure at ambient temperature for 24 h.

A Philips/FEI XL30 ESEM operating at 25 kV was used to investigate the polyHIPE morphology. Fractured polyHIPE pieces were sputter-coated with gold using a Bio-Rad E5400 sputter coating system and mounted on carbon fibre pads adhered to aluminium stubs. Average void diameters were then calculated using Image J Version 1.50i. One hundred voids were randomly chosen from an SEM image of the sample and the diameters measured. Void diameters measured in this way underestimate the true value as the voids are unlikely to be exactly bisected. Therefore a statistical correction factor was used to account for this underestimate.<sup>14</sup>

### **Sample Collection and Processing**

Endometrial biopsies were obtained from patients attending the Implantation Clinic, a dedicated research clinic at University Hospitals Coventry and Warwickshire (UHCW) NHS Trust, Coventry, UK. All research was undertaken with NHS National Research Ethics Committee approval (1997/5065). All biopsies were retrieved from the Arden Tissue Bank at UHCW. All participants provided written informed consent in accordance with the guidelines of the Declaration of Helsinki, 2000. Separation and purification of HEECs and HESCs were performed as described previously in detail.<sup>15</sup>

## 2D and 3D Primary Cultures

PolyHIPE discs (15 mm diameter and 400  $\mu\text{m}$  thickness) were placed in 24-well plates, disinfected with 100 % ethanol, rendered hydrophilic with 70 % ethanol, and washed twice with sterile phosphate buffered saline (PBS). The polyHIPE scaffolds were then coated with fibronectin (300  $\mu\text{L}$ ; 0.33 mg/mL in PBS solution was used for each scaffold) to improve cell adherence. The scaffolds were left in the fibronectin solution for 1 h at ambient temperature and then used without further washing. A suspension of  $2.5 \times 10^5$  HEECs in 50  $\mu\text{L}$  conditioned reprogramming of epithelial cell (CRC) medium was carefully added onto the centre of each scaffold disc and incubated for 1 h at 37 °C. A 2 mL CRC medium was then added to each well and the plate was maintained at 37°C in a 5% CO<sub>2</sub> humidified environment. Media were changed every other day. The CRC medium was made up of the following reagents: 500 mL DMEM/F12 with phenol red (Thermo Fisher Scientific, Gibco™, catalog number: 31330-038), 50 mL DCC (dextran-coated charcoal-treated fetal bovine serum), 2 mM L-glutamine, 5  $\mu\text{g/mL}$  Insulin, 5 mL Antibiotic-Antimycotic solution (100 X) 5 mL, 8.4 ng/mL cholera toxin, 10 ng/mL EGF, 0.4  $\mu\text{g/mL}$  hydrocortisone, 24  $\mu\text{g/mL}$  adenine, 10  $\mu\text{M/L}$  Y-27632 (Merck Millipore). Primary HESCs in 2D and 3D cultures were grown in DMEM/F12 medium with phenol red (Gibco, Fisher Scientific, Loughborough, UK), supplemented 10% dextran-coated charcoal-treated fetal bovine serum (DCC-FBS), 10  $\mu\text{M}$  L-glutamine (Gibco), 1  $\times$  Antibiotic Antimycotic (Gibco), 1 nM  $\beta$ -estradiol and 2  $\mu\text{g/ml}$  recombinant human insulin (Sigma-Aldrich, Poole, UK). The cultures were maintained in 37°C in a 5% CO<sub>2</sub> humidified environment and the culture medium was refreshed every 48 h. For differentiation experiments, cells, grown either as a monolayer or in 3D scaffolds, were exposed to DMEM/F-12 containing 2% DCC-FBS with 0.5 mM 8-bromo-cAMP (Sigma-Aldrich) and  $10^{-6}$  M medroxyprogesterone acetate (MPA; Sigma-Aldrich) for either 3 or 7 days.



### **Haematoxylin-Eosin (H&E) Staining**

Media were aspirated from the wells. PolyHIPE scaffolds were washed twice with 2 mL PBS and transferred to a 5 mL plastic vial containing 4 % formaldehyde. Formaldehyde fixed discs were processed and embedded in paraffin. Sections (5  $\mu$ m) were obtained using a microtome, mounted on a glass slide and left to dry at 60 °C overnight. Slides were re-hydrated by a sequence of 3 baths of xylene for 5 minutes each, followed by 2 baths of 100 % isopropanol for 2 minutes each. Slides were then dipped in 70 % isopropanol for 2 minutes and rinsed in distilled water for 2 minutes. Slides were incubated with filtered haematoxylin for 1 minute and rinsed with warm running tap water for 15 minutes. They were placed in distilled water for 30 seconds and in 95% ethanol for 30 seconds. Cells were counterstained with eosin-Y for 1 minute. To dehydrate and clear the sections, slides were immersed in a sequence of 2 baths of 95% ethanol, 2 bath of 100% ethanol and 2 baths of xylene (2 minutes each). Coverslips were applied to the slides using distyrene/plasticizer/xylene (DPX) mounting medium.

### **Immunostaining**

Formaldehyde-fixed scaffolds were processed and embedded in paraffin and 5  $\mu$ m sections were obtained using a microtome. Sections were mounted onto glass slides and left to dry at 60 °C overnight. Slides were re-hydrated by a sequence of 3 baths of xylene for 5 minutes each, followed by 2 baths of 100 % isopropanol for 2 minutes each. Slides were then dipped in 70 % isopropanol for 2 minutes, rinsed in distilled water for 2 minutes, dipped in 10 mM citrate buffer pH 6.0, and

placed in an epitope retriever unit for 2 hours. For immunostaining, Novolink Polymer Detection System (Leica) was used. Peroxidase Block was added for 5 minutes, and 0.05 % polysorbate 20 (Tween 20) in tris buffered saline (TBS-T) was used twice for washing. Sections were incubated overnight at 4 °C in primary antibodies diluted in 0.05 % TBS-T. The slides were again rinsed twice with TBS-T and incubated with Post Primary Block for 30 minutes. Two more 0.05 % TBS-T washes were carried out and the slides were incubated for 30 minutes with Novolink Polymer Solution. Slides were rinsed with 0.05 % TBS-T, incubated for 5 minutes with diaminobenzidine chromogen and rinsed with water for 5 minutes. Slides were counterstained with haematoxylin. The primary antibodies, cytokeratin 18 (Abcam; AB668) and vimentin (Cell Signalling, 3390) were diluted 1:1000.

### **Immunofluorescence and Confocal Microscopy**

Cell monolayers were grown in glass-bottom Petri-dishes until 80-90 % confluent. Cells in scaffolds were cultured for 7 days. Culture media were aspirated and cells were washed in PBS and fixed in 4 % formaldehyde. Formaldehyde was aspirated and cells were washed with PBS for 5 minutes. Cells were permeabilized with 0.1 % Triton X-100 for 1 h at room temperature, washed with PBS for 5 minutes and incubated in 1% BSA / PBS (v/v) for 1 h to block nonspecific binding of antibodies. Cells were incubated overnight with primary antibodies diluted 1/100 in 1% (w/v) BSA/PBS at 4 °C, washed with 1% BSA/PBS and incubated with secondary antibodies diluted 1/200 in 1 % BSA/PBS at 4 °C for 2 h in the dark. A new 1% BSA / PBS wash was carried out, and cells were coverslipped with mounting medium containing DAPI for nuclear counterstaining. The cells were imaged using a confocal microscope (Zeiss LSM 710). Confocal images were

captured with a 488 nm wavelength scanning laser and emitted light recorded through a band-pass filter (505–530 nm).

### **RNA Isolation from Cells in Culture**

Cells in culture were washed twice with PBS. After the addition of phenol-guanidinium thiocyanate monophasic solution (Stat-60) (AMS Biotechnology), cells were harvested by scraping. A 20 % volume of ice-cold chloroform was added to RNase-free Eppendorf tubes containing homogenates and vigorously vortexed for 15 seconds. Tubes were centrifuged at 4 °C at 16,000 g for 30 minutes. The aqueous phase that contains the RNA remains was separated from the organic phase (at the bottom) that contains DNA and proteins and transferred to RNase-free Eppendorf tubes containing half of the original STAT-60 volume of ice-cold isopropanol and 20 µg glycogen. After being thoroughly vortexed, tubes were stored at -80 °C for at least 30 min (maximum 24 h) to precipitate the RNA. Tubes were thawed on ice and centrifuged at 4 °C at 16,000 g for 15 minutes. RNA pellets were washed twice with 500 µL of 75 % (v/v) ethanol in RNase free-water, and allowed to dry for 2 minutes, before resuspension in TE buffer pH 8.0. RNA concentration and purity were measured using a spectrophotometer. RNA purity was considered satisfactory when the absorbance ratio at 260/280  $\geq 1.8$ .

### **Complementary DNA (cDNA) Synthesis from mRNA**

A reverse transcription kit (Qiagen) was used for cDNA synthesis. 1 µg of template RNA, 2 µL of 7 x gDNA Wipeout buffer and nuclease-free water to complete 14 µL were mixed in pre-chilled

RNAse-free Eppendorf tubes. Tubes were vortexed, centrifuged briefly and incubated at 42 °C for 2 min to remove the genomic DNA. 4 µL RT buffer (5×), 1 µL RT Primer Mix and 1 µL Quantiscript Reverse Transcriptase were added to each tube, vortexed, and briefly centrifuged. Control sample without the reverse transcriptase was prepared, using 1 µL of water instead of the enzyme. Tubes were incubated at 42 °C for 30 minutes. In order to inactivate the reverse transcriptase, tubes were incubated at 95 °C for 3 minutes. Final cDNA was diluted 1/5 by adding 80 µL nuclease free-water. Samples were assayed immediately or stored at – 20 °C.

### **Real-Time Quantitative PCR (RT-qPCR)**

Total RNA was extracted from 2D and 3D cultures using RNA STAT-60 (AMS Biotechnology). Equal amounts of total RNA were treated with DNase and reverse transcribed using the QuantiTect Reverse Transcription Kit (QIAGEN) and the resulting cDNA used as template in RT-qPCR analysis. Detection of gene expression was performed with Power SYBR® Green Master Mix and the 7500 Real Time PCR System. The expression levels of the samples were calculated using the dCt method, incorporating the efficiencies of each primer pair. The variances of input cDNA were normalised against the levels of the *L19* housekeeping gene. All measurements were performed in triplicate. Melting curve analysis confirmed product specificity. Primer sequences used were as follows: *L19* forward 5'-GCG GAA GGG TAC AGC CAA-3', *L19* reverse 5'-GCA GCC GGG CGC AAA-3'; *PRL* forward 5'-AAG CTG TAG AGA TTG AGG AGC AAA C-3', *PRL* reverse 5'-TCA GGA TGA ACC TGG CTG ACT A-3'; *PAEP* forward 5'-GAG CAT GAT GTG CCA GTA CC-3', *PAEP* reverse 5'-tga tga atc cct gca tga tctc-3'; *DPP4* forward 5'-CCA AAG ACT GTA CGG GTT CC-3', *DPP4* reverse 5'-ACA AAG AAC TTT ACA GTT GGA TTC AC-3'.

## RNA Sequencing and Data Analysis

Total RNA was extracted using RNA-STAT-60 from primary cultures. Four biological repeat experiments were performed to allow for inter-biopsy variability. RNA quality was analysed on an Agilent 2100 Bioanalyzer. RNA integrity number score for all samples was  $\geq 8.0$ . Library preparations were performed by Warwick Genomics Facility. Ovation RNASeq System V2® (Nugen Technologies) was used for cDNA synthesis and amplification. First strand cDNA was prepared using a DNA/RNA chimeric primer mix and reverse transcriptase. This resulted in cDNA/mRNA hybrid molecules containing a RNA sequence at the 5' end of the cDNA strand. Priming sites for DNA polymerase were created by fragmenting the mRNA within the cDNA/mRNA complex, in order to synthesise a second DNA strand. Next the cDNA was amplified using DNA/RNA chimeric SPIA primers and DNA polymerase. RNA in the 5' end of the cDNA strand was removed from the hybrid molecule by RNase H. The libraries were sent to Wellcome Trust Centre for Human Genomics (Oxford, UK) for pair-end next generation sequencing using Illumina HiSeq and with a reading length of 100 base pairs, producing 150 million pair reads. Transcriptomic maps of paired-end reads were generated using Bowtie-2.2.6,<sup>16</sup> SAMtools 1.2,<sup>17</sup> and TopHat 2.1.0 against the hg19 reference transcriptome (2014) using the firststrand setting. Transcript counts were assessed by HTSeq-0.6.1<sup>18</sup> and transcripts per million (TPMs) were calculated as recently described.<sup>19</sup> Differential gene expression analysis was performed using DEseq2-1.14.1.<sup>20</sup> Significance was defined as an adjusted *P* value (*q* value) of  $<0.05$  after Bonferroni multiple testing correction. Gene Ontology (GO) analyses were carried out using DAVID Bioinformatics Resources 6.8.<sup>21</sup>

## Statistical Analysis

Data were analysed with the statistical package Graphpad Prism v6 (Graphpad software Inc, La Jolla, CA, USA). Student's *t*-test was used when appropriate. Statistical significance was assumed at  $P < 0.05$ .

## RESULTS AND DISCUSSION

Well-defined polyHIPE materials derived from trimethylolpropane tris(3-mercaptopropionate) (TMPTMP) and dipentaerythritol penta-/hexa-acrylate (DPEHA) were prepared using emulsion templating and thiol-acrylate photopolymerization, as reported previously.<sup>9</sup> The typical interconnected open-cell morphology of polyHIPE materials was confirmed by scanning electron microscopy (SEM), Figure 1A. Highly interconnected porous materials have great potential as scaffolds for 3D cell culture and in tissue engineering applications as they allow effective nutrient and waste transport to and from the cells. This is an attractive advantage of polyHIPE scaffolds over other 3D cell culture systems, such as hydrogels where poor media diffusion may restrict nutrient supply to cells. Void diameter distribution of the material was determined by analysis of SEM images, Figure 1B. The average void diameter of the polyHIPE material was found to be ca. 25  $\mu\text{m}$ , which is likely sufficient for most cell types to infiltrate the scaffold. PolyHIPE scaffolds have been previously used to support the growth of a wide range of cell types including chondrocytes,<sup>22</sup> osteoblasts,<sup>23</sup> keratinocytes,<sup>24</sup> hepatocytes,<sup>25</sup> and neurons;<sup>26</sup> nevertheless, to the

best of our knowledge this is the first report of primary human endometrial cells grown on polyHIPE scaffolds.

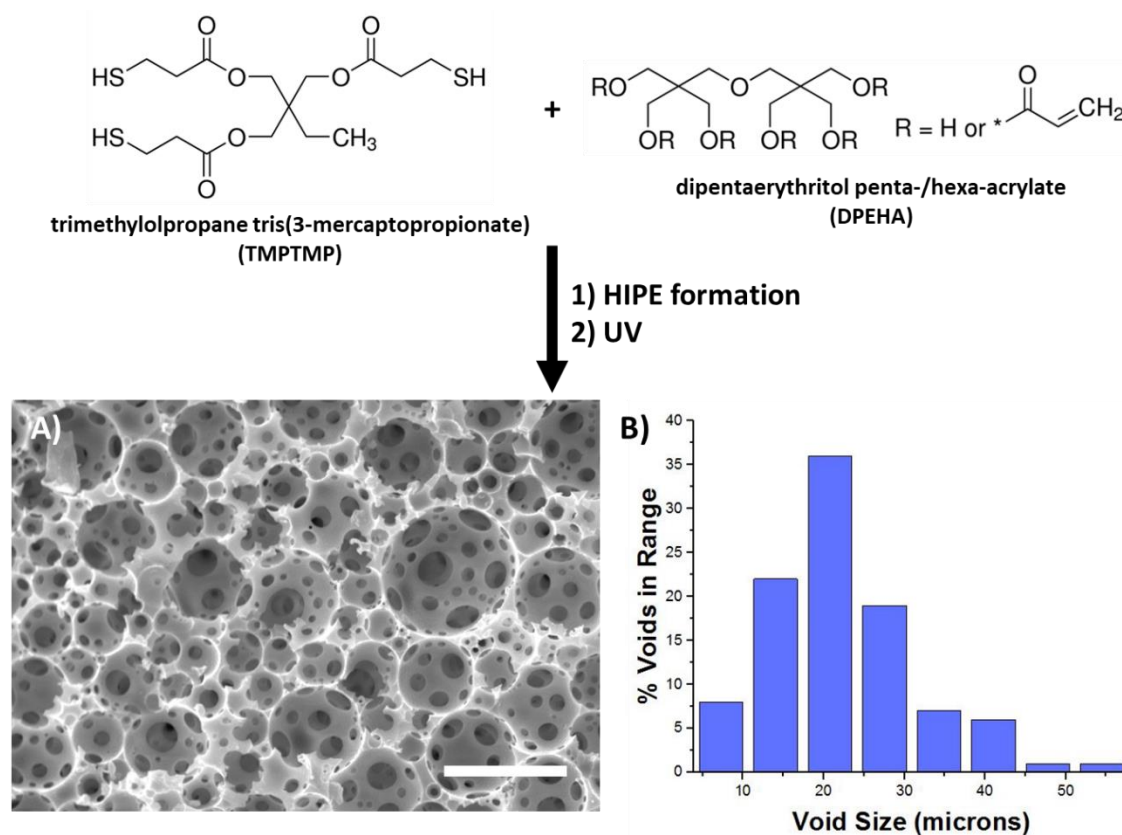


**Figure 1.** Synthesis of polyHIPEs from TMPTMP and DPEHA. A) SEM micrograph of a polyHIPE material and B) Void diameter distribution determined by analysis of SEM image. Scale bar = 50  $\mu\text{m}$ .

We hypothesized that polyHIPE scaffolds would create a more physiologically relevant 3D environment for the growth of endometrial cells compared to conventional 2D monolayer culture, consistent with a preliminary study that reported on an electrospun polymer scaffold for primary

bovine endometrial cell culture.<sup>27</sup> However, electrospun scaffolds possess disadvantages, limiting their applications for routine use. In electrospun scaffolds, 3D growth is restricted to the nodes where fibres overlap which can prevent extensive organisation. More importantly, electrospun scaffolds suffer from poor mechanical properties, unlike polyHIPE scaffolds that are more mechanically robust.<sup>11</sup>

The produced cylindrical polyHIPE monoliths were sectioned using a vibrating-blade microtome into membranes of about 400  $\mu\text{m}$ , 15 mm in diameter, allowing membranes to be placed in 24-well plates, Figure 2. Transwell® inserts were applied (after removing the polycarbonate membrane) to prevent scaffolds from floating when media is added. Fully submerged scaffolds were expected to offer cells maximum nutrient supply as media could access the cells from above and below. It has been reported that the use of extracellular matrix (ECM) glycoproteins enables cell attachment to synthetic substrates such as polystyrene.<sup>28</sup> We therefore investigated the effect of coating of polyHIPE scaffolds with fibronectin (one of the most abundant ECM proteins) on the endometrial cell adhesion onto the polyHIPE material.

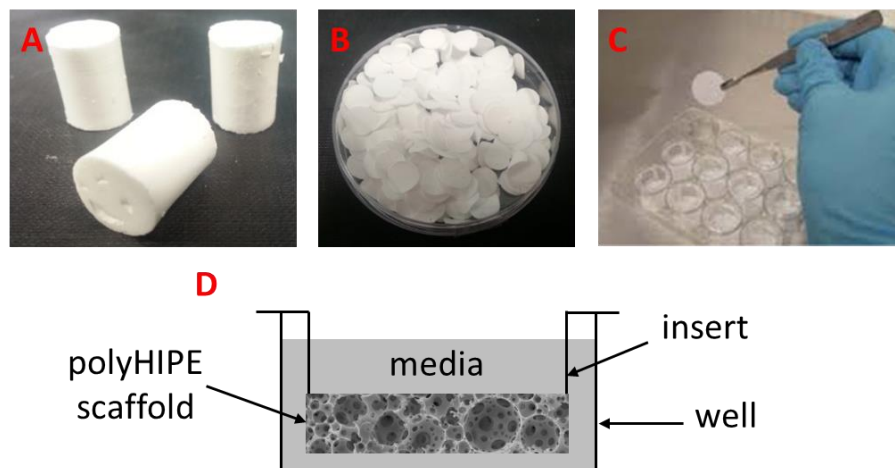




**Figure 2.** Photographs of polyHIPE A) monoliths, B) discs of 400  $\mu\text{m}$  thickness and C) inserted in cell culture well-plate. D) Presentation of a fully submerged polyHIPE scaffold in culture media using a Transwell® insert.

Adhesion and growth of HEECs and HESCs was assessed at days 2, 7 and 15. After 2 days in culture, more cells were adhered onto the surface of the fibronectin-coated scaffolds when compared to uncoated scaffolds, Figure 3 and 4. Consequently, fibronectin coating of scaffolds was performed routinely in all subsequent experiments. As the culture period progresses to 7 and 15 days, cells remained healthy with no overt signs of cell loss or apoptosis. Although further migration into the scaffold was modest, the cells retained their phenotype (Figure 5), suggesting that the polyHIPE material provides a suitable environment for maintaining cells in prolonged cultures. Unlike primary cells, polyHIPE scaffolds were readily colonised when seeded with Ishikawa cells, an endometrial adenocarcinoma cell line widely used as a cell model that recapitulates endometrial receptivity for embryo implantation,<sup>29</sup> Figure 6. Therefore, further optimisation of scaffold architecture and/or culture conditions is necessary to improve primary cell penetration and proliferation.

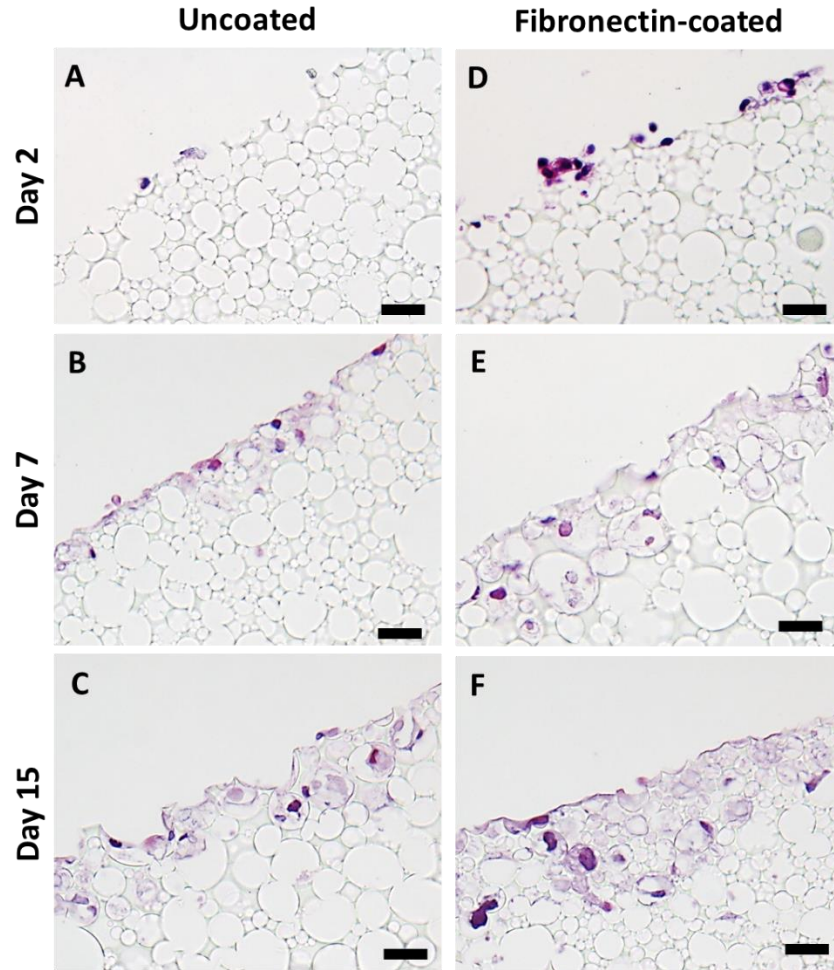


**Figure 3.** H & E staining of HEEC growth in polyHIPE scaffolds using 24-well plate format. (A,D) Day 2. (B,E) Day 7. (C,F) Day 15. Scaffolds were either left uncoated (A,B,C) or coated with fibronectin (D,E,F). Cell seeding density =  $2.5 \times 10^5$ . Fibronectin coating modestly promotes cell adhesion and migration into the material. Scale bars = 50  $\mu\text{m}$

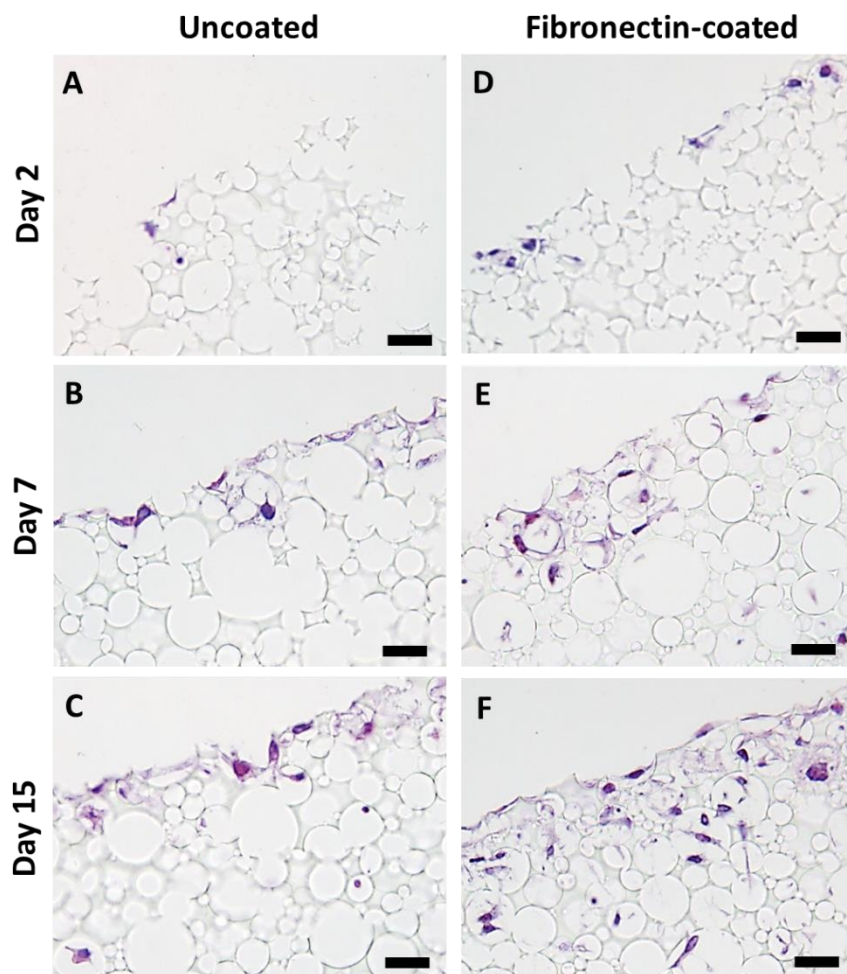


**Figure 4.** H & E staining of HESC growth in polyHIPE scaffolds using 24-well plate format. (A,D) Day 2. (B,E) Day 7. (C,F) Day 15. Scaffolds were either left uncoated (A,B,C) or coated with fibronectin (D,E,F). Cell seeding density =  $2.5 \times 10^5$ . Fibronectin seems to help cell adhesion and encourages penetration into the material. Scale bars = 50  $\mu\text{m}$

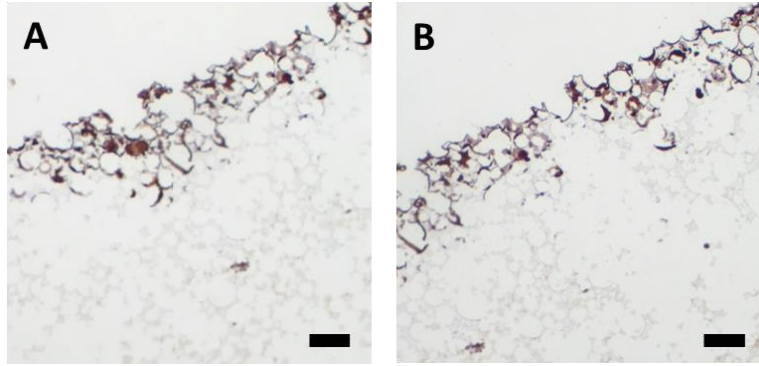


**Figure 5.** A) HEECs stained with an epithelial marker, CK18 and B) HESCs stained with a stromal marker, Vimentin, grown in polyHIPE scaffolds for 15 days. Scale bars = 50  $\mu\text{m}$ .

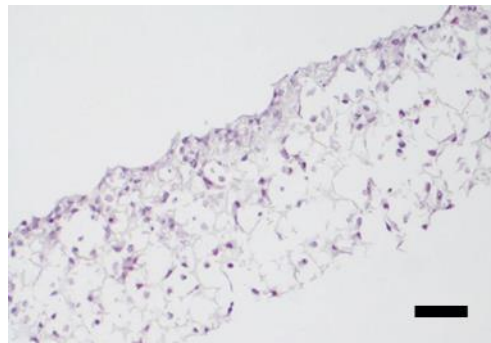


**Figure 6.** H & E stained Ishikawa cells grown in a polyHIPE scaffold for 15 days. Cell seeding density =  $2.5 \times 10^5$ . Scale bar = 100  $\mu\text{m}$

In a monolayer culture (2D), HEECs and HESCs exhibited a flattened and often distorted morphology with limited evidence of cell-cell contact. It is recognised that limited cell-cell and cell-ECM interaction would lead to rapid loss of phenotype and native function.<sup>30</sup> Importantly, HEECs and HESCs cultured in scaffolds were more rounded, displaying a distinct 3D

configuration akin to the native cell morphology found *in vivo*, Figure 7. The topology of the scaffold is expected to keep cells in their native 3D morphology and hence increase cell-cell contact.

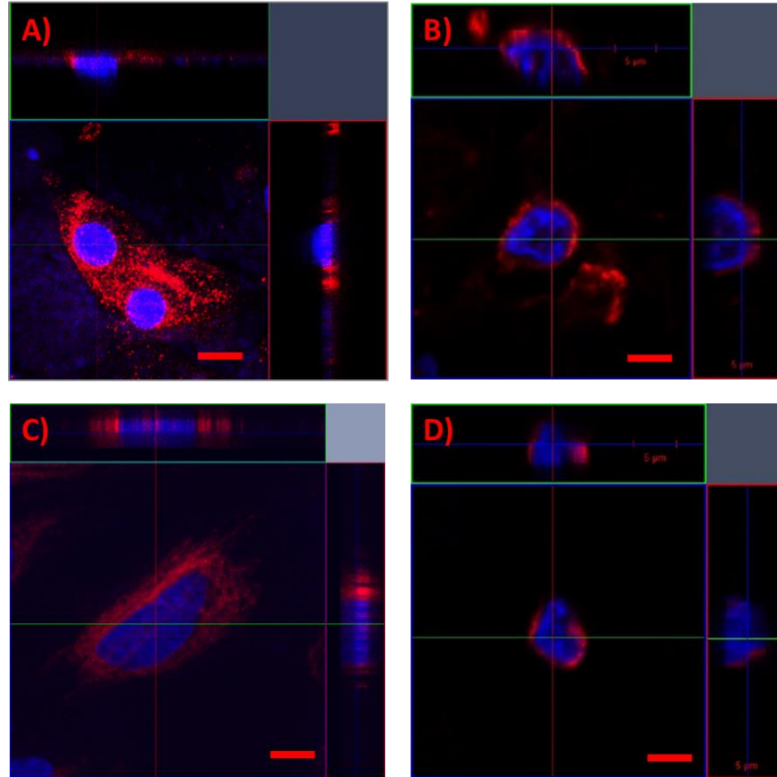


**Figure 7.** Laser scanning confocal micrographs of cultured HEECs A) in 2D; B) in polyHIPE scaffold and HESCs C) in 2D; D) in polyHIPE scaffold. Immunofluorescence staining of HEECs by anti-CK18 antibody/DAPI and HESCs by anti-vimentin antibody/DAPI. Scale bars = 5  $\mu\text{m}$ .

To characterize the transcriptome differences between cells grown in polyHIPE scaffolds and in monolayer cultures, we performed RNA sequencing. HEECs isolated from 4 different biopsies

were cultured in parallel on polyHIPE scaffolds and as a monolayer until 80-90 % confluent. Total RNA was extracted and subjected to RNA sequencing with approximately 33-47 million paired-end reads sequenced per sample. Although variation in gene expression was observed between cultures from different biopsies, Principal components 1 and 2 accounted for 47% and 22% of variance in gene expression, respectively, clearly distinguishing the impact of the different culture conditions, Figure 8 A. After accounting for variation between primary cultures, the impact of 2D versus 3D culture conditions was highly significant. Based on  $q < 0.05$ , 495 genes were found to be differentially expressed between the culture systems, (Figure 8 B) with 289 and 206 genes significantly enriched in monolayer and polyHIPE scaffold cultures, respectively (Table S1, Supporting Information).

To identify the biological processes impacted by the culture conditions, Gene Ontology (GO) analysis was performed. Genes upregulated in polyHIPE scaffold cultures were highly enriched for functional categories related to extra-cellular matrix deposition (GO:0031012,  $P < 2.58E-12$ ) and cell adhesion (GO:0007155,  $P < 2.39E-4$ ) (Table S2, Supporting Information). Notably, gene ontology categories related to positive regulation of cell division (GO:0051781,  $P < 0.028$ ) were also enriched in polyHIPE cultures, suggesting an advantage of HEECs grown in polyHIPE scaffolds over 2D cultures. By contrast, downregulated genes in polyHIPE scaffold cultures included multiple 1 interferon-responding genes (IRGs), resulting in enriched for functional categories related to defence response to virus (GO:0051607  $< 2.19E-17$ ) (Table S3, Supporting Information).

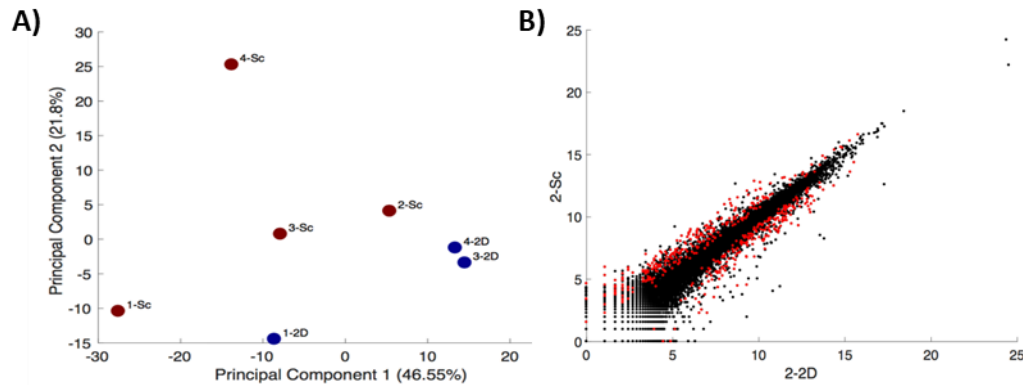


**Figure 8.** Identification of genes differentially expressed in scaffold vs 2D cultures samples. A) Principal component analysis segregates paired HEESCs grown on polyHIPE scaffold (n=4; red dots) and in standard 2D cultures (n=4; blue dots). Principal components 1 and 2 account for >68% of variation in gene expression. B) Scatterplot of log transformed gene expression in representative polyHIPE scaffold and monolayer RNA sequencing libraries. Red dots indicate significant differentially expressed genes.

Embryo attachment to and invasion into the endometrium is dependent on differentiation of both epithelial and stromal cell populations and expression of evolutionarily conserved receptivity genes. In humans, transformation of the stroma into a decidual matrix that governs trophoblast invasion and placenta formation is initiated in response to the postovulatory surge in progesterone and rising cellular cyclic adenosine monophosphate (cAMP) levels.<sup>31</sup> The induction of a receptive phenotype in primary endometrial cells in response to culturing conditions was assessed in two ways. First, expression of *PAEP*, which encodes progestagen-associated endometrial protein, was compared between 2D and 3D cultures of HEECs cultured for either 3 or 7 days. *PAEP* is highly expressed in the endometrium during the window of implantation. When compared to a 2D

monolayer, HEECs grown on scaffolds expressed higher transcript levels for *PAEP*, Figure 9A. Furthermore, the ability of HEECs to differentiate into specialized decidual cells in response to 8-bromo-cAMP and MPA signalling was also enhanced in 3D, as exemplified by higher induction on day 7 of culture of *PRL*, a cardinal decidual marker gene, Figure 9B.

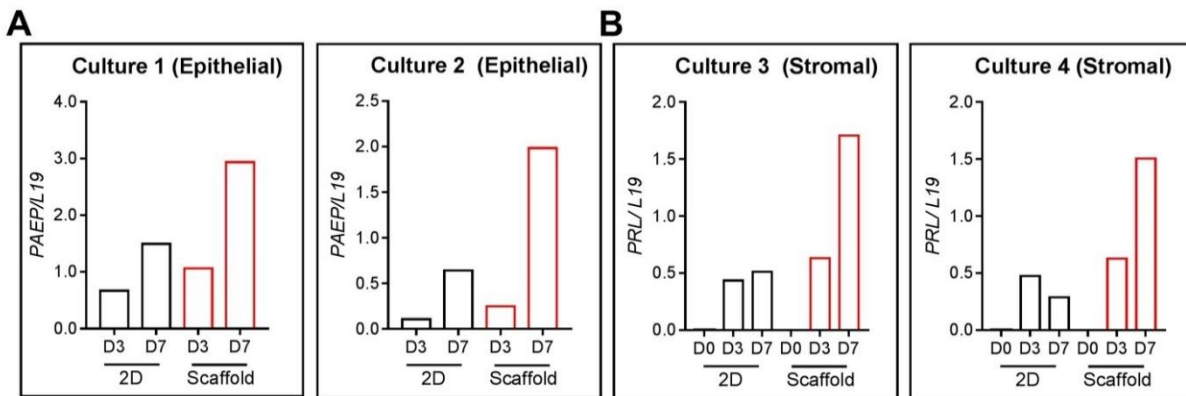


**Figure 9.** Expression of endometrial differentiation markers in primary endometrial cells grown in 3D versus 2D cultures : A) *PAEP* mRNA levels in HEECs, cultured either as a monolayer (2D) or in scaffolds, were measured after 3 or 7 days of culture by RTQ-PCR. *PAEP* mRNA levels were normalized to the housekeeping gene *L19* and expressed as arbitrary units (a.u.). The data show expression in two primary HEEC cultures established from different biopsies. B) Induction of decidual *PRL* expression in HEECs cultures as monolayers or in scaffolds. Parallel cultures either remained untreated (D0, control) or were decidualized using 8-bromo-cAMP and MPA for 3 or 7 days. Total mRNA was harvested and subjected to RTQ-PCR. *PRL* mRNA levels were normalized to the housekeeping gene *L19*. The data show induction of *PRL* in two independent primary cultures.



## CONCLUSIONS

A well-defined polyHIPE material was prepared by emulsion templating and thiol-ene photopolymerization techniques. The morphology of this material was found to be fully interconnected, highly porous and supports the *in vitro* 3D growth of primary human endometrial cells. Preliminary cell culture experiments showed that both HEECs and HESCs adhere on the polyHIPE scaffold and that the material is sufficiently open to allow cell infiltration, although further optimisation is needed to allow full cell population of the scaffold. Differentiation experiments and morphological transcriptomic analyses demonstrated that polyHIPE scaffolds can offer a more physiologically relevant growth environment for endometrial cells *in vitro* compared to monolayer cultures. Cells grown in scaffolds displayed higher expression levels of PAEP, a gene involved in conferring endometrial receptivity to implantation, and a much enhanced ability to differentiate into specialised decidual cells in response to 8-bromo-cAMP and MPA. We therefore believe that polyHIPE materials could form the foundation for development of a functional, representative 3D model of human endometrium that will be advantageous for the study of miscarriage or implantation failure; and aid the development of novel therapeutic strategies. Furthermore, because of the ability to allow cell expansion in 3D culture, we envisage that degradable polyHIPE materials may be useful in medical applications, such as autologous organ reconstruction.

## ASSOCIATED CONTENT

**Supporting Information.** The following files are available free of charge.

**Table S1.** Differential expressed genes between 2D and Scaffold cultures. Genes sorted according to p-value and enrichment in Scaffold over 2D; **Table S2.** Gene ontology analysis for genes enriched in Scaffold over 2D (Bonferroni adjusted p-value < 0.05); **Table S3.** Gene ontology analysis for genes enriched in 2D over Scaffold (Bonferroni adjusted p-value < 0.05) (Microsoft Excel Worksheet (.xlsx))

## AUTHOR INFORMATION

### Corresponding Author

\*(A.M.E.) E-mail: a.m.eissa@warwick.ac.uk

\*(J.J.B.) E-mail: j.j.brosens@warwick.ac.uk

\*(N.R.C.) E-mail: neil.cameron@monash.edu

### Author Contributions

The manuscript was written through contributions of all authors. All authors have given approval to the final version of the manuscript.

### Notes

The authors declare no competing financial interest.

## ACKNOWLEDGMENT

We would like to thank the Monash-Warwick Alliance for financial support. This work was funded in part by a National Institute for Health Research Blood and Transplant Research Unit (NIHR BTRU) in red cell products in partnership with NHS Blood and Transplant. The views expressed are those of the author(s) and not necessarily those of the NHS, the NIHR or the Department of Health.

## REFERENCES

- (1) Aplin, J. D.; Ruane, P. T., Embryo-epithelium interactions during implantation at a glance. *J. Cell Sci.* **2017**, 130, (1), 15-22.
- (2) Bongso, A.; Gajra, B.; Lian, N. P.; Wong, P. C.; Soonchye, N.; Ratnam, S., Establishment of human endometrial cell-cultures. *Hum. Reprod.* **1988**, 3, (6), 705-713.
- (3) Valentijn, A. J.; Saretzki, G.; Tempest, N.; Critchley, H. O. D.; Hapangama, D. K., Human endometrial epithelial telomerase is important for epithelial proliferation and glandular formation with potential implications in endometriosis. *Hum. Reprod.* **2015**, 30, (12), 2816-2828.
- (4) ClassenLinke, I.; Kusche, M.; Knauth, R.; Beier, H. M., Establishment of a human endometrial cell culture system and characterization of its polarized hormone responsive epithelial cells. *Cell Tissue Res.* **1997**, 287, (1), 171-185.
- (5) Carnachan, R. J.; Bokhari, M.; Przyborski, S. A.; Cameron, N. R., Tailoring the morphology of emulsion-templated porous polymers. *Soft Matter* **2006**, 2, (7), 608-616.
- (6) Hayward, A. S.; Eissa, A. M.; Maltman, D. J.; Sano, N.; Przyborski, S. A.; Cameron, N. R., Galactose-functionalized polyhipec scaffolds for use in routine three dimensional culture of mammalian hepatocytes. *Biomacromolecules* **2013**, 14, (12), 4271-4277.

- (7) Paljevac, M.; Gradisnik, L.; Lipovsek, S.; Maver, U.; Kotek, J.; Krajnc, P., Multiple-Level Porous Polymer Monoliths with Interconnected Cellular Topology Prepared by Combining Hard Sphere and Emulsion Templating for Use in Bone Tissue Engineering. *Macromol. Biosci.* **2018**, *18*, 1700306.
- (8) Lovelady, E.; Kimmins, S. D.; Wu, J. J.; Cameron, N. R., Preparation of emulsion-templated porous polymers using thiol-ene and thiol-yne chemistry. *Polym. Chem.* **2011**, *2*, (3), 559-562.
- (9) Caldwell, S.; Johnson, D. W.; Didsbury, M. P.; Murray, B. A.; Wu, J. J.; Przyborski, S. A.; Cameron, N. R., Degradable emulsion-templated scaffolds for tissue engineering from thiol-ene photopolymerisation. *Soft Matter* **2012**, *8*, (40), 10344-10351.
- (10) Johnson, D. W.; Langford, C. R.; Didsbury, M. P.; Lipp, B.; Przyborski, S. A.; Cameron, N. R., Fully biodegradable and biocompatible emulsion templated polymer scaffolds by thiol-acrylate polymerization of polycaprolactone macromonomers. *Polym. Chem.* **2015**, *6*, (41), 7256-7263.
- (11) Chen, C. Y.; Eissa, A. M.; Schiller, T. L.; Cameron, N. R., Emulsion-templated porous polymers prepared by thiol-ene and thiol-yne photopolymerisation using multifunctional acrylate and non-acrylate monomers. *Polymer* **2017**, *126*, 395-401.
- (12) Lee, A.; Langford, C. R.; Rodriguez-Lorenzo, L. M.; Thissen, H.; Cameron, N. R., Bioceramic nanocomposite thiol-acrylate polyHIPE scaffolds for enhanced osteoblastic cell culture in 3D. *Biomater. Sci.* **2017**, *5*, (10), 2035-2047.
- (13) Murphy, A. R.; Ghobrial, I.; Jamshidi, P.; Laslett, A.; O'Brien, C. M.; Cameron, N. R., Tailored emulsion-templated porous polymer scaffolds for iPSC-derived human neural precursor cell culture. *Polym. Chem.* **2017**, *8*, (43), 6617-6627.

- (14) Barbetta, A.; Cameron, N. R., Morphology and surface area of emulsion-derived (PolyHIPE) solid foams prepared with oil-phase soluble porogenic solvents: Span 80 as surfactant. *Macromolecules* **2004**, 37, (9), 3188-3201.
- (15) Barros, F. S., Brosens, J. J. and Brighton, P. J., Isolation and primary culture of various cell types from whole human endometrial biopsies. *Bio-protocol* **2016**, 6, (22), e2028.
- (16) Langmead, B.; Salzberg, S. L., Fast gapped-read alignment with Bowtie 2. *Nat. Methods* **2012**, 9, (4), 357-9.
- (17) Li, H.; Handsaker, B.; Wysoker, A.; Fennell, T.; Ruan, J.; Homer, N.; Marth, G.; Abecasis, G.; Durbin, R., The sequence alignment/map format and samtools. *Bioinformatics* **2009**, 25, (16), 2078-9.
- (18) Anders, S.; Pyl, P. T.; Huber, W., HTSeq--a Python framework to work with high-throughput sequencing data. *Bioinformatics* **2015**, 31, (2), 166-9.
- (19) Anders, S.; Huber, W., Differential expression analysis for sequence count data. *Genome Biol.* **2010**, 11, (10), R106.
- (20) Love, M. I.; Huber, W.; Anders, S., Moderated estimation of fold change and dispersion for RNA-seq data with DESeq2. *Genome Biol.* **2014**, 15, (12), 550.
- (21) Huang da, W.; Sherman, B. T.; Lempicki, R. A., Systematic and integrative analysis of large gene lists using DAVID bioinformatics resources. *Nat. Protoc.* **2009**, 4, (1), 44-57.
- (22) Naranda, J.; Susec, M.; Maver, U.; Gradisnik, L.; Gorenjak, M.; Vukasovic, A.; Ivkovic, A.; Rupnik, M. S.; Vogrin, M.; Krajnc, P., Polyester type polyHIPE scaffolds with an interconnected porous structure for cartilage regeneration. *Sci. Rep.* **2016**, 6.
- (23) Akay, G.; Birch, M. A.; Bokhari, M. A., Microcellular polyHIPE polymer supports osteoblast growth and bone formation in vitro. *Biomaterials* **2004**, 25, (18), 3991-4000.

- (24) Sharma, R.; Barakzai, S. Z.; Taylor, S. E.; Donadeu, F. X., Epidermal-like architecture obtained from equine keratinocytes in three-dimensional cultures. *J. Tissue Eng. Regen. Med.* **2016**, 10, (8), 627-636.
- (25) Hayward, A. S.; Sano, N.; Przyborski, S. A.; Cameron, N. R., Acrylic-acid-functionalized polyhipec scaffolds for use in 3d cell culture. *Macromol. Rapid Commun.* **2013**, 34, (23-24), 1844-1849.
- (26) Hayman, M. W.; Smith, K. H.; Cameron, N. R.; Przyborski, S. A., Growth of human stem cell-derived neurons on solid three-dimensional polymers. *J. Biochem. Biophys. Methods* **2005**, 62, (3), 231-240.
- (27) MacKintosh, S. B.; Serino, L. P.; Iddon, P. D.; Brown, R.; Conlan, R. S.; Wright, C. J.; Maffei, T. G. G.; Raxworthy, M. J.; Sheldon, I. M., A three-dimensional model of primary bovine endometrium using an electrospun scaffold. *Biofabrication* **2015**, 7, (2).
- (28) Kleinman, H. K.; Klebe, R. J.; Martin, G. R., Role of collagenous matrices in the adhesion and growth of cells. *J. Cell Biol.* **1981**, 88, (3), 473-485.
- (29) Somkuti, S. G.; Yuan, L. W.; Fritz, M. A.; Lessey, B. A., Epidermal growth factor and sex steroids dynamically regulate a marker of endometrial receptivity in Ishikawa cells. *J. Clin. Endocrinol. Metab.* **1997**, 82, (7), 2192-2197.
- (30) Baker, B. M.; Chen, C. S., Deconstructing the third dimension - how 3D culture microenvironments alter cellular cues. *J. Cell Sci.* **2012**, 125, (13), 3015-3024.
- (31) Gellersen, B.; Brosens, J. J., Cyclic decidualization of the human endometrium in reproductive health and failure. *Endocr. Rev.* **2014**, 35, (6), 851-905.

## TABLE OF CONTENTS GRAPHIC

